

<https://doi.org/10.1038/s42003-025-07930-2>

PTOV1 interacts with ZNF449 to promote colorectal cancer development



Zhiyong Wang^{1,5}, Xinwei Qiao^{2,5}, Kaming Xue³, Qianzhi Chen⁴✉ & Anshu Li¹✉

PTOV1 is recognized to have a significant role in various human cancers, including prostate cancer. However, it remains unclear what its clinical significance and biological role are in colorectal cancer (CRC). TCGA, NCBI/GEO, and Kaplan–Meier plot database mining provided important clues into the function and clinical importance of PTOV1 in CRC. Western blotting, immunohistochemistry, and immunofluorescence were utilized to discover PTOV1 protein levels in CRC cell lines and tissues. To explore the involvement of PTOV1 in the development of CRC and the underlying mechanisms, several in-vitro and in-vivo studies were executed, such as CCK-8 assays, colony formation, transwell assays, qRT-PCR, Co-IP, GST pull-down, immunostaining, and mouse xenograft assays. It was shown that PTOV1 expression level was upregulated in the tissues and cells of human CRC. PTOV1 high-expression level was associated with short survival. ZNF449 interacted with PTOV1 and accelerated CRC development in vitro and in vivo. Through Co-IP and GST pull-down studies, the physical interaction of PTOV1/ZNF449 was demonstrated. Furthermore, PTOV1 directly bound ZNF449, and this complex synergistically promoted the transcription of MYC. In addition, the PTOV1/ZNF449 interaction was disrupted by the TAT-PTOV1 (125–283 aa) protein leading to inhibit the CRC development in a xenografted mouse model. According to these findings, PTOV1 has an essential role in CRC progression, and PTOV1/ZNF449 interaction could be a possible therapeutic target for CRC.

Colorectal cancer (CRC) is considered one of the major prevalent malignant cancers, which rise every year worldwide, and the health and lives of humans are gravely threatened by it¹. CRC is still the fourth greatest cause of death globally despite therapeutic advances in the last decade². It is urgent that new therapeutic approaches be found for CRC, which is marked by uncontrolled cellular proliferation.

In a differential display technique for screening of overexpressed genes in prostate cancer, prostate tumor overexpressed-1 (PTOV1) was specified as a new gene and protein. In a 12-exon gene restricted to chromosome 19q13.3, this protein was encoded³. In the carcinoma and intraepithelial neoplasia of prostate, PTOV1 is overexpressed but cannot be detected or expressed at lower levels of healthy prostate cells. In prostate tumors, PTOV1 levels were significantly correlated with Ki67 proliferative index and related to the proteins' nuclear localization⁴. As well as co-localizing at the plasma membrane and in the nucleus, PTOV1 reacts with the lipid rafts protein flotillin-1. Under basal conditions, PTOV1 depletion significantly inhibited cell proliferation⁵. The non-small cell lung cancer cells were

proven as sensitive to chemotherapy when PTOV1 is depleted, as reported by Wu et al.⁶ revealing the role of PTOV1 in tumor progression.

This study explored the impact of PTOV1 on the development of CRC. PTOV1 expression was overexpressed in human CRC. Mechanistically, PTOV1 was found to interact with ZNF449 to synergistically enhance the transcription of MYC to promote CRC development. In addition, the PTOV1/ZNF449 interaction, which disrupted, decreased the development of xenografted CRC in nude mice.

Results

PTOV1 expression is overexpressed in human CRC

In order to screen specifically highly expressed protein molecules in CRC tumor tissues, we utilized high-throughput sequencing to determine the differences in the protein expression in three paired healthy colorectal and CRC tissues. The findings demonstrated that PTOV1 was particularly highly expressed in tumor specimens (Fig. S1A). To further validate the PTOV1 expression in CRC tissues, we employed western blotting (WB) to

¹Department of Gastrointestinal Surgery, Union Hospital, Tongji Medical College, Huazhong University of Science and Technology, Wuhan, Hubei, China.

²Department of Thoracic Surgery, Union Hospital, Tongji Medical College, Huazhong University of Science and Technology, Wuhan, Hubei, China. ³Department of Traditional Chinese Medicine, Union Hospital, Tongji Medical College, Huazhong University of Science and Technology, Wuhan, Hubei, China. ⁴Department of Breast and Thyroid Surgery, Union Hospital, Tongji Medical College, Huazhong University of Science and Technology, Wuhan, Hubei, China. ⁵These authors contributed equally: Zhiyong Wang, Xinwei Qiao. ✉e-mail: simonsk2008@hust.edu.cn; anshuli@163.com

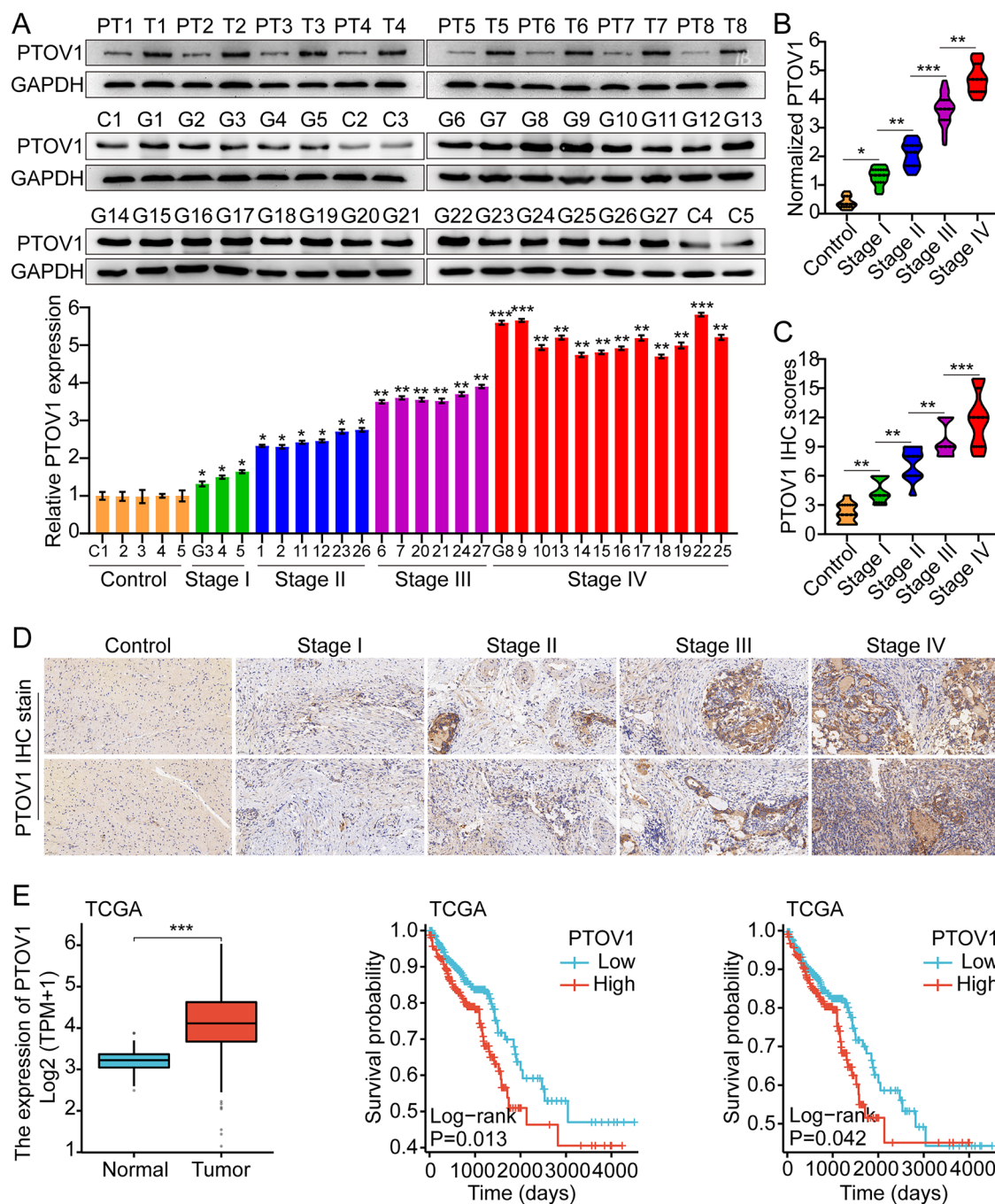


Fig. 1 | PTOV1 expression is overexpressed in human CRC. **A** PTOV1 levels in paired paracancerous (PT1-8) and tumor tissues (T1-8); in normal intestinal tissue (C1-5) and CRC tissues (Stage I, G3-5; Stage II, G1-2, 11, 12, 23 and 26; Stage III, G7, 20-21, 24 and 27; Stage IV, G8-10, 13-19, 22 and 25). GAPDH was an internal control. **B** RT-PCR of PTOV1 in normal and CRC tissues. Relative PTOV1 expression is normalized to that of the C1 sample. Three different portions of samples were examined. **C**, **D** IHC staining and scoring were used to detect the

protein levels of PTOV1 in CRC tissues and normal tissues. Bars: 50 μ m. **E** The expression of PTOV1 in CRC tissues compared with normal tissues and the Kaplan-Meier analysis of survival in CRC in TCGA database. The means \pm SDs are provided ($n = 3$). * $P < 0.05$, ** $P < 0.01$, and *** $P < 0.001$ according to two-tailed Student t-tests or one-way ANOVA followed by Dunnett tests for multiple comparisons.

identify the expression level of PTOV1 in eight cases of paired tumor tissues and surrounding tissues. The findings revealed that PTOV1 was greatly expressed in tumor specimens. In addition, we detected 5 cases of normal colorectal tissues and 27 cases of CRC tumor tissues of different grades by WB, and the findings again presented that tumor tissues had high PTOV1 expression, especially in high-grade CRC (Fig. 1A). In addition, we utilized qRT-PCR to identify ten cases of normal colorectal tissues and CRC tissues of different grades (20 stage I, 30 stage II, 56 stage III, and 12 stage IV). The

findings also revealed that, compared to normal colorectal tissues, PTOV1 was highly expressed in CRC, particularly in high-grade CRC (Fig. 1B). At the same time, we used IHC to identify the PTOV1 expression in the above tissues and used the previous method to score the IHC, and the results supported the above conclusions again (Fig. 1C, D). Moreover, we investigated the connection between PTOV1 levels and the survival of patients between various grades of CRC in public databases of patient specimens. The results revealed PTOV1 was overexpressed significantly in human CRC

tissues compared to healthy colorectal tissues; furthermore, higher PTOV1 expressions were correlated with poorer survival (Figs. 1E and S1B).

The ROC analysis was performed between PTOV1-based, TNM-based, and a combination of both to predict clinical outcomes in order to evaluate the pathological and clinical predictive value of PTOV1. As evaluated by the area under the curve (AUC), the combination model performed better than the TNM-based model alone (0.752), (0.642). It appears that the combination of PTOV1 and TNM stage could more accurately predict clinical results than the TNM stage alone (Fig. S1C–D). Additionally, we investigated the relationship between PTOV1 mRNA levels and clinicopathological features in 118 CRC tissues. Table S1 reveals the clinical, pathological, and tumor molecular characteristics in accordance with the PTOV1 mRNA expression level. The findings demonstrated that PTOV1 mRNA expression was significantly linked to tumor size ($P < 0.0001$), lymph node metastasis ($P < 0.0001$), and TNM stage ($P = 0.0011$). Moreover, univariate and multivariate Cox regression analyses revealed that elevated PTOV1 mRNA expression level was an independent predictor for poor survival among CRC patients (Table S2). Table S2 reveals that a higher PTOV1 mRNA expression level is related to TNM stage and lymph node metastasis. These findings indicated that PTOV1 could be a potential biomarker for CRC.

Overexpression of PTOV1 facilitates tumor cell growth

The first step was to measure PTOV1 protein in two normal intestinal epithelium cells (FHC and HIEC-6) and six CRC cell lines (SW1116, SW48, HCT-15, SW620, SW480, and SW1463) by WB. According to the results, PTOV1 protein levels are higher in the CRC cell line than in normal intestinal epithelium cells (Fig. S1E). Therefore, we selected two cell lines, SW48 and SW620, with moderate expression of PTOV1 protein for subsequent research. Next, WB verified the overexpressed PTOV1 in SW48 and SW620 cells (Fig. S1G). Our next step was to determine PTOV1 impacts on CRC cell development, migration, and invasion using CCK-8, colony formation, Flow Cytometry Experiment, WB, and Transwell experiments. The findings revealed that PTOV1 overexpression stimulated CRC cell growth, migration, and invasion (Fig. 2A–C). Flow cytometry results showed that overexpression of PTOV1 inhibited cell apoptosis and promoted cell cycle progression (Fig. S2A). Furthermore, in vivo animal experiments once again showed that overexpression of PTOV1 promotes tumor growth. Ki-67 IF staining was conducted to determine the tumor's proliferation index. This further suggested that proliferation in the PTOV1 upregulation group was greater than in the control group (Fig. 2D). These findings suggest that the upregulation of PTOV1 promotes tumor growth.

Knockdown of PTOV1 suppresses tumor cell growth

Next, PTOV1 was knocked down in SW48 and SW620 cells, and the knockdown efficiency was confirmed utilizing WB (Fig. S1F). As the si-PTOV1#2 with the highest knockdown efficiency, it will be used as a follow-up study. To define the impacts of PTOV1 on tumor development, migration, and invasion, we used CCK-8, colony formation, Flow Cytometry Experiment, WB, TUNEL, and Transwell experiments. The findings illustrated that PTOV1 knockdown inhibited tumor cell growth, migration, and invasion (Fig. 3A–C). Flow cytometry results showed that knockdown of PTOV1 promoted cell apoptosis and inhibited cell cycle progression (Fig. S2B). Of course, in order to present more comprehensive analysis of protumorigenic effect of PTOV1 in OE and KO cells, we used WB to detect key EMT markers. The results showed that overexpression of PTOV1 downregulated E-cadherin, a marker of epithelial cell characteristics, and upregulated N-cadherin and Vimentin, markers of mesenchymal cell characteristics, while knockdown of PTOV1 showed the opposite effect (Fig. S3A). In addition, the results of TUNEL experiments also showed that overexpression of PTOV1 inhibited cell apoptosis, while knockdown of PTOV1 promoted cell apoptosis, which was consistent with the trend of flow cytometry results (Fig. S3B). Furthermore, in vivo animal experiments once

again showed that PTOV1 knockdown inhibits tumor growth. Ki-67 IF staining was conducted to evaluate the proliferative index of tumor, which suggested that proliferation was reduced in the PTOV1 knockdown group compared to the control group (Fig. 3D). In addition, we also used immunohistochemistry to detect the expression level of PTOV1 in the subcutaneous tumors of animals in different treatment groups, and the results once again confirmed that our treatment was effective (Fig. S3B). These data suggest that the knockdown of PTOV1 suppresses tumor growth.

Identification of PTOV1 Binding Proteins in CRC Cells

To gain a deeper understanding of PTOV1 downstream signaling, we conducted Co-IP and mass spectrometry (MS). In order to characterize PTOV1 binding partners, we performed a protein analysis report (Fig. 4A). The PTOV1 intracellular domain was utilized to minimize the binding candidates from SW48 cell lysate. We then electrophoresed and analyzed the mass spectra of precipitates (Fig. 4B). Here we are also based on the characteristic tradition of our laboratory because we have been committed to studying MYC, so we screened the interacting molecules of PTOV1 based on two considerations, one is that it can directly bind to the MYC promoter region as a transcription factor, and the other is that it can bind to PTOV1. Combining the predictions of the online database UCSC and JASPA database, using the Venn diagram to take the intersection, we found that only ZNF449 and ZNF185 met the requirements, but Co-IP confirmed that ZNF185 could not bind to PTOV1 (Fig. S3C). Among the important binding proteins, we finally chose ZNF449 to further study its interaction with PTOV1 based on comprehensive analysis. Furthermore, in the cultured SW48 lysates and SW620 cells, the endogenous interaction of PTOV1 with ZNF449 was detected by Co-IP and GST pull-down. The data indicate that PTOV1 reacts with ZNF449 in CRC cells (Fig. 4C, D). Also, we investigated whether PTOV1 and ZNF449 co-localized with CRC cells. IF staining revealed coexpression of PTOV1 and ZNF449 in CRC cells (Fig. 4E). Additionally, immunohistochemistry revealed that PTOV1 was widely coexpressed with ZNF449 in CRC tissues (Fig. 4F). The above results all indicate that PTOV1 can directly bind ZNF449.

According to the secondary structure predicted using the InterPro (<http://www.ebi.ac.uk/interpro/>), PDB (<https://www.rcsb.org/>), and Pfam (www.pfam.org) databases, we created three truncations of PTOV1 to verify its binding to ZNF449. Co-IP and GST pull-down assays revealed that the ZNF449-specific binding sequences were spotted in the 125–283 aa region of PTOV1 protein (Fig. S4). Of course, to confirm further the expression of ZNF449 in CRC tissues, we utilized WB to determine ZNF449 expression level in 4 cases of paired tumor tissues and adjacent tissues. The outcomes presented that ZNF449 was highly expressed in tissues of the tumor. Moreover, the data based on TCGA data analysis indicated that PTOV1 was highly expressed in tissues of the tumor relative to healthy tissues (Fig. S5A–B).

Disruption of PTOV1/ZNF449 Interaction Slows the CRC progression

Figure S4 presents that PTOV1 (125–283 aa) was critical for mediating the interaction between PTOV1 and ZNF449. We further investigated whether PTOV1 (125–283 aa) could affect the interaction between PTOV1 and ZNF449. We prepared PTOV1 (125–283 aa) protein tagged with TAT peptide. Using TAT protein (10 μ M), the Flag-PTOV1 and HA-ZNF449 fusion proteins were incubated. Then, the Co-IP assay was performed. The TAT protein significantly reduced the amount of ZNF449 bound to PTOV1, indicating that the TAT-PTOV1 (125–283 aa) protein can affect the interaction of PTOV1/ZNF449 in vitro.

To validate the impact of TAT-PTOV1 (125–283 aa) protein on the endogenous PTOV1/ZNF449 interaction, we investigated if the TAT protein could be transferred into the CRC cells (Fig. S5C). SW48 and SW620 cells were supplemented by TAT protein for 20 min as described previously⁷

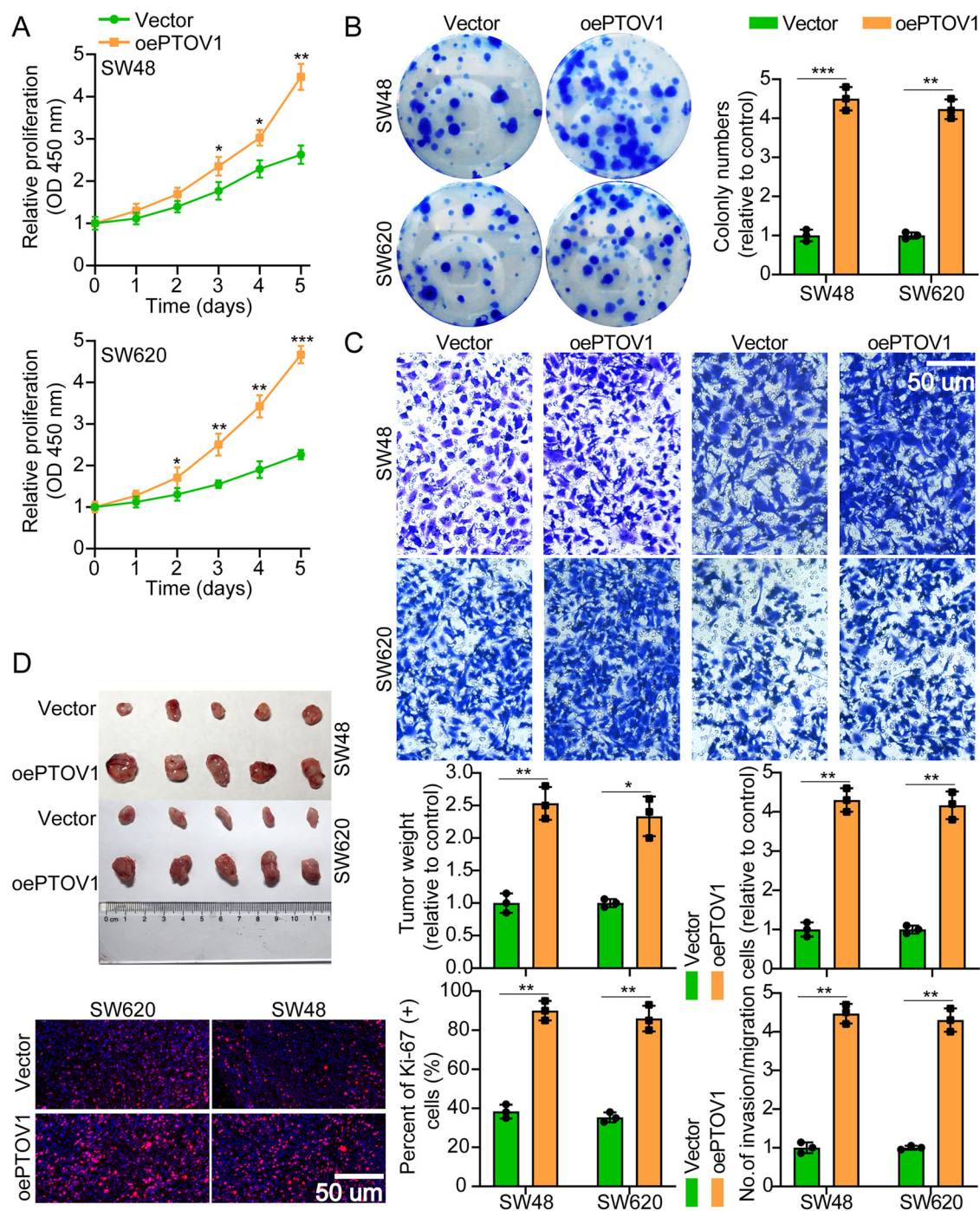


Fig. 2 | Overexpression of PTOV1 facilitates tumor cell growth. A Cell growth curves measured by CCK-8 between Vector and oePTOV1. **B** PTOV1 overexpression facilitated colony formation and histogram quantification (panels). **C** Transwell assays showing that overexpression of PTOV1 facilitates cell migration and invasion. The numbers of migration and invading cells are shown. Bars: 50 μ m.

D Typical pictures of subcutaneous tumor between Vector and oePTOV1. Representative pictures of Ki-67 staining between Vector and oePTOV1. Bars: 50 μ m. The means \pm SDs are provided ($n = 3$). * $P < 0.05$, ** $P < 0.01$, and *** $P < 0.001$ according to two-tailed Student t-tests or one-way ANOVA followed by Dunnett tests for multiple comparisons.

and prepared for immunostaining with antibodies against TAT. The TAT motif promoted the delivery of PTOV1 (125–283 aa) protein into SW48 and SW620 cells. Next, we investigated whether the TAT-PTOV1 (125–283 aa) protein could affect the connection between PTOV1/ZNF449 in CRC cells. TAT protein (0.2 μ M) was incubated with SW48 and SW620 cells for 20 min. Then, IP with anti-Flag-PTOV1 and anti-HA-ZNF449 was performed on the cell lysates. The interaction of PTOV1/ZNF449 in the CRC cells was significantly diminished by performing the TAT-PTOV1 (125–283 aa) protein (Fig. S5D).

To further identify the impact of TAT-PTOV1 (125–283 aa) protein on the CRC cells, CCK-8 and colony formation assays were conducted. TAT-PTOV1 (125–283 aa) protein incubation obviously suppressed the proliferation capability of CRC cells (Fig. S5E–F). These results indicated that TAT-PTOV1 (125–283 aa) protein seems to reduce CRC cell proliferation. Transwell experiments data also demonstrated that TAT-PTOV1 (125–283 aa) protein could weaken CRC cell migration and invasion (Fig. S6A). Furthermore, in vivo animal experiments once again showed that TAT-PTOV1 (125–283 aa) protein could inhibit tumor growth. Staining of Ki-67

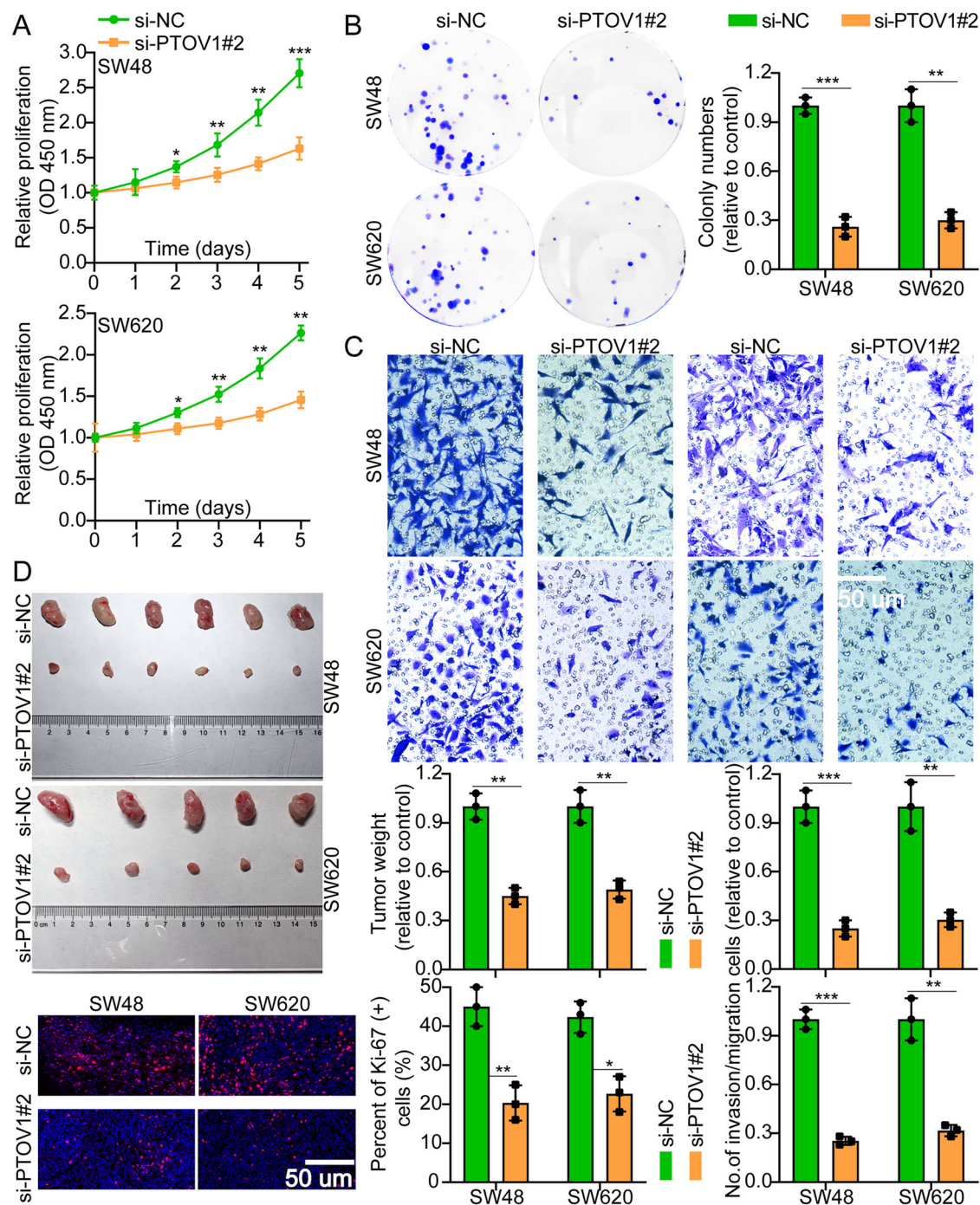


Fig. 3 | Knockdown of PTOV1 suppresses tumor cell growth. **A** Cell growth curves measured by CCK-8 assay between si-NC and si-PTOV1#2. **B** PTOV1 over-expression inhibited colony formation and histogram quantification (panels). **C** Transwell assays showing that PTOV1 knockdown inhibits cell migration and invasion. The numbers of migration and invading cells are shown. Bars: 50 μ m.

D Typical pictures of subcutaneous tumor between si-NC and si-PTOV1#2. Representative pictures of Ki-67 staining between si-NC and si-PTOV1#2. Bars: 50 μ m. The means \pm SDs are provided ($n = 3$). * $P < 0.05$, ** $P < 0.01$, and *** $P < 0.001$ according to two-tailed Student t-tests or one-way ANOVA followed by Dunnett tests for multiple comparisons.

IF was conducted to evaluate the proliferative index of tumor, which also suggested that proliferation in the TAT-PTOV1 (125–283 aa) protein group was reduced in comparison with the control group (Fig. S6B). These data suggest that disruption of PTOV1/ZNF449 interaction slows the CRC progression.

PTOV1 promotes ZNF449-mediated transcription of MYC

The expression of target genes is controlled by transcription factors that bind to DNA-specific sequences. Using the JASPAR database⁸, we

discovered that ZNF449 could significantly bind to the MYC promoter region. To demonstrate that MYC is a target for transcription of ZNF449 and that the regulation can be promoted by PTOV1, Wild-type (WT) or mutant (mut) MYC promoter luciferase vectors were constructed and transfected into SW48 and SW620 cells (Fig. 5A). The luciferase assay demonstrated that upregulation of ZNF449 induced WT MYC promoter activity, as indicated by an increase in luciferase activity, but overexpression had no effect on the activity of mut-type MYC promoter. Moreover, PTOV1 enhanced the rise in luciferase activity stimulated by ZNF449 (Fig. 5B). We

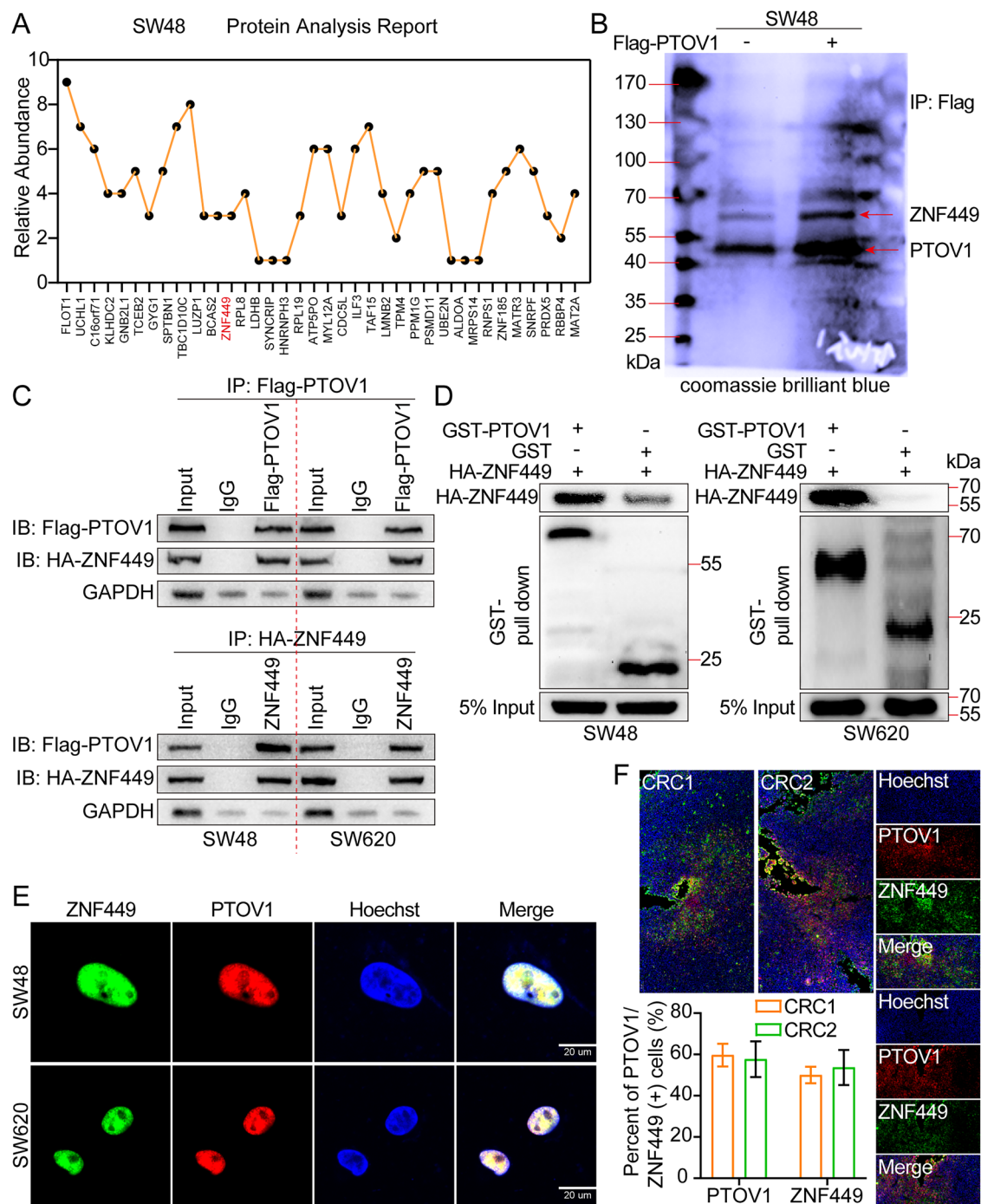


Fig. 4 | Identification of PTOV1 Binding Proteins in CRC Cells. **A** Protein analysis report to characterize PTOV1 binding partners. **B** Identification of PTOV1-binding proteins by WB and MS. **C, D** Using Co-IP and GST pull-down to clarify that

PTOV1 can directly bind ZNF449. **E** IF staining revealed coexpression of PTOV1 and ZNF449 in CRC cells. Bars: 20 μ m. **F** IF staining showed the colocalization (yellow) between ZNF449 (green) and PTOV1 (red) in CRC sections. Bars: 50 μ m.

also performed the ChIP assay, and the outcomes showed that ZNF449 was restricted by the MYC promoter, and PTOV1 enhanced this interaction (Fig. 5C). Furthermore, the enhanced expression of ZNF449 significantly overexpressed the level of MYC mRNA and protein, both of which were further promoted by PTOV1 (Fig. 5D). Interestingly when we mutated the binding site of PTOV1 on ZNF449, we found that Δ PTOV1 failed to enhance the rise in luciferase activity stimulated by ZNF449 (Fig. S6C), enhance the binding of ZNF449 to the promoter region of MYC (Fig. S7A) or potentiate ZNF449 upregulation of MYC mRNA and protein (Figs. S6D and S7B). Furthermore, we investigated the relationship between MYC levels and patient survival across different grades of CRC in accessible

patient specimen databases. The results revealed MYC was significantly overexpressed in human CRC specimens compared to normal colorectal specimens; furthermore, higher MYC expressions were correlated with poorer survival (Fig. S7C). These findings showed that ZNF449 bound directly to the promoter region of MYC for activation of transcription, and PTOV1 promotes this process.

PTOV1 promotes tumor growth through ZNF449

First, ZNF449 was knocked down in SW48 and SW620 cells, and the WB confirmed the efficiency of knockdown (Fig. S7D). As the si-PTOV1#2 with the highest knockdown efficiency, it will be used as a

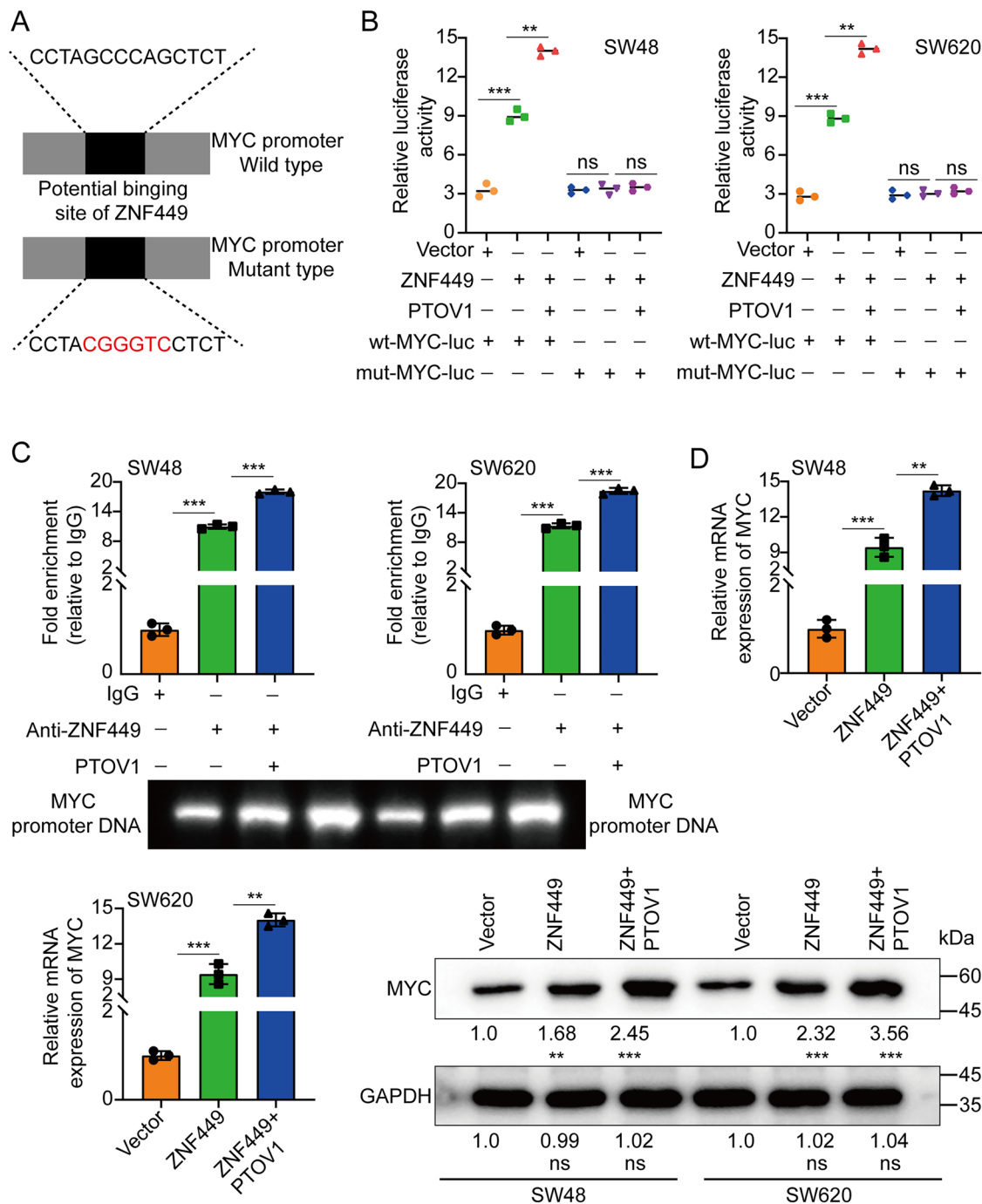


Fig. 5 | PTOV1 promotes ZNF449-mediated transcription of MYC. **A** We constructed the wild-type or mutant-type luciferase vectors based on the potential binding site of ZNF449 to the MYC promoter. **B** Luciferase activity was assayed in SW48 and SW620 cells transfected with luciferase vectors (wild type or mutant type) and meantime co-transfected with expression plasmids (empty vectors, ZNF449 expression plasmids, or PTOV1 expression plasmids). **C** ChIP experiments of

ZNF449 (IgG as an internal control) were performed, and the co-precipitated DNA was subjected to PCR amplification with primers specific to MYC promoter region. **D** The level of MYC under ectopic expression of ZNF449 or PTOV1 was detected by qRT-PCR and WB. The means \pm SDs are provided ($n = 3$). ** $P < 0.01$ and *** $P < 0.001$ according to two-tailed Student t-tests or one-way ANOVA followed by Dunnett tests for multiple comparisons. ns, no significant difference.

follow-up study. In order to further verify that PTOV1 promotes tumor growth by regulating ZNF449. We knocked down ZNF449 while overexpressing PTOV1 and used CCK-8, colony formation, TUNEL, and Transwell assays. The outcomes revealed that PTOV1 upregulation promoted tumor cell growth, migration, and invasion; however, the knockdown of ZNF449 could reduce the enhancement of tumor cell proliferation, migration, and invasion caused by PTOV1 upregulation (Fig. 6A–C). Furthermore, in vivo animal

experiments once again showed that PTOV1 overexpression promoted tumor cell growth. The proliferative index of tumor was evaluated by performing staining to Ki-67 IF, which also suggested that proliferation was greater in the PTOV1 overexpression group than in the control group. However, the knockdown of ZNF449 could attenuate the above phenomenon (Fig. 6D). In addition, TUNEL assay results showed that overexpression of PTOV1 inhibited cell apoptosis, while knockdown of ZNF449 weakened the above effect

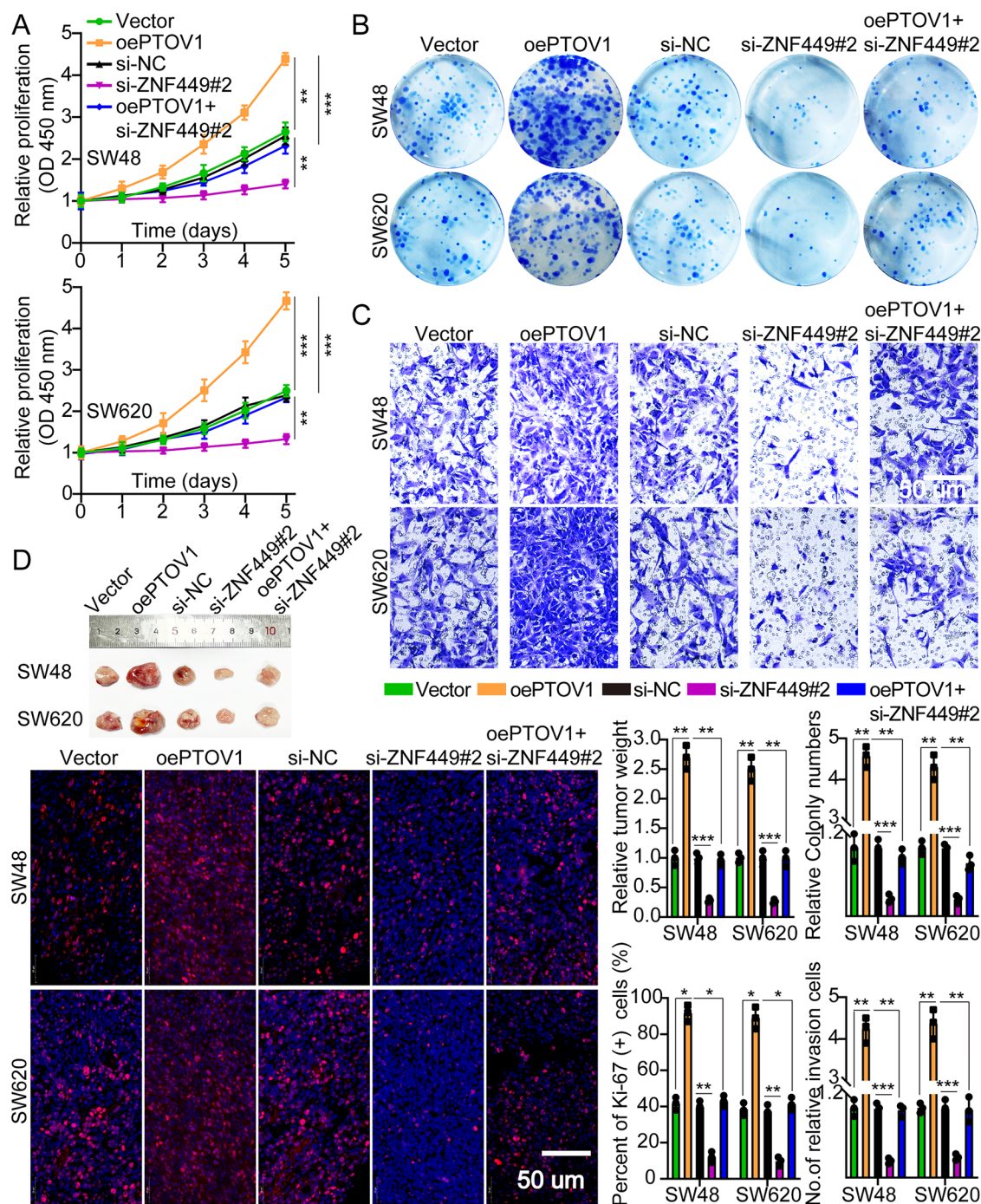


Fig. 6 | PTOV1 promotes tumor growth through ZNF449. **A** Cell growth curve measured by CCK-8 assay between Vector, oePTOV1, si-NC, si-ZNF449#2, and oePTOV1+si-ZNF449#2. **B** PTOV1 overexpression promoted colony formation and the effect could be attenuated by knock down ZNF449. **C** Transwell assays showing that PTOV1 overexpression promoted tumor cell invasion and the effect could be attenuated by knock down ZNF449. The numbers of invading cells are

shown. Bars: 50 μ m. **D** Typical pictures of subcutaneous tumor between Vector, oePTOV1, si-NC, si-ZNF449#2, and oePTOV1+si-ZNF449#2. Bars: 50 μ m. The means \pm SDs are provided ($n = 3$). * $P < 0.05$, ** $P < 0.01$, and *** $P < 0.001$ according to two-tailed Student t-tests or one-way ANOVA followed by Dunnett tests for multiple comparisons.

(Figure S8A). At the same time, we also used immunohistochemistry to detect the expression levels of PTOV1/ZNF449/MYC in the subcutaneous tumors of animals in different treatment groups. The experimental data once again confirmed that our treatment was effective (Fig. S8B-C). In addition, we also used WB to detect the expression level of MYC in subcutaneous tumors of animals in different treatment groups. The experimental results were completely consistent with the results of immunohistochemistry (Fig. S9A).

These data suggest that PTOV1 promotes tumor growth through ZNF449.

PTOV1 promotes tumor growth through MYC

First, MYC was knocked down in SW48 and SW620 cells, and the efficiency of knockdown was confirmed utilizing WB (Fig. S7D). As the si-MYC#2 with the highest knockdown efficiency, it will be used as a follow-up study. In order to further verify that PTOV1 promotes tumor growth by regulating

MYC. We knocked down MYC while overexpressing PTOV1 and used CCK-8, colony formation, and Transwell assays. The findings revealed that overexpression of PTOV1 promoted tumor cell growth, migration, and invasion; however, knockdown of MYC could reduce the enhancement of tumor cell growth, migration, and invasion caused by overexpression of PTOV1 (Fig. 7A–C). Furthermore, in vivo, animal experiments once again showed that PTOV1 overexpression promoted tumor cell growth Ki-67 IF staining was conducted to determine the tumor proliferation index, which revealed that growth in overexpression of PTOV1 group was greater than that of the control group. However, the knockdown of MYC could attenuate the above phenomenon (Fig. 7D). These data suggest that PTOV1 promotes tumor growth through MYC.

PTOV1 is directly targeted by HIF-1 α

Hypoxia serves as a key environmental factor in CRC, regularly contributing to invasion, metastasis, and malignancy. Transcription factors often bind to particular DNA sequences to control gene expression. Analysis with the JASPAR database showed that HIF-1 α binds to the promoter of the PTOV1 gene. To clarify how HIF-1 α regulates PTOV1 transcription, luciferase vectors with either wild-type or altered PTOV1 promoters were created and introduced into SW48 and SW620 cells (Fig. S9B). According to the luciferase assay, the activity of the wild-type (WT) PTOV1 promoter was increased by upregulating HIF-1 α , as shown by elevated luciferase activity. Conversely, the overexpression of HIF-1 α had no impact on the activity of the mutant PTOV1 promoter (Fig. S9C). Moreover, ChIP assays showed that HIF-1 α binds to the PTOV1 promoter (Fig. S9D). HIF-1 α overexpression caused a notable rise in the levels of PTOV1 mRNA and protein (Fig. S9E). The above experimental results show that HIF-1 α directly binds to the promoter region of PTOV1, thereby promoting the transcriptional activity and expression level of PTOV1.

Correlation of the PTOV1/ZNF449/MYC axis with clinical progression

The PTOV1/ZNF449/MYC expression levels among normal colorectal tissue (Control), Stage I, Stage II, Stage III, and Stage IV were measured. Compared to the expression level in Control, there was a higher expression of PTOV1/ZNF449/MYC in tumor tissues, especially in Stage IV (Figs. 1B and 8A, B). Additionally, the expression levels of members of the PTOV1/ZNF449/MYC signaling axis were directly proportional to one another (Fig. 8C–E). Of course, IF outcomes revealed that the PTOV1 levels were positively associated with ZNF449/MYC signaling (Fig. 8F).

Discussion

PTOV1 was found and considered to be upregulated in prostate cancer first³. Later, high levels of PTOV1 were found to be associated with a worse prognosis for prostate cancer⁹, breast cancer¹⁰, urothelial carcinoma¹¹, lung cancer⁶. However, the PTOV1 role in CRC has not been thoroughly examined. As a result of analyzing data from NCBI/ GEO and TCGA microarray databases, we revealed that PTOV1 was consistently overexpressed in cancer tissues compared to controls. In addition, we used WB, qRT-PCR, IHC, and IF to identify the level of expression of PTOV1 in clinical tumor and normal control samples from different cohorts, and the findings verified the high expression of PTOV1 in tumor samples. Moreover, our results from qRT-PCR and statistical analyses of a cohort of CRC specimens revealed that PTOV1 was an independent and weak prognostic factor. The survival time of individuals with a higher PTOV1 level was shorter than that of individuals with a lower PTOV1.

According to a recent investigation, Verónica et al. revealed that transduction of PTOV1 significantly increased the survival rate of tumor cells after docetaxel exposure and enhanced the expression level of docetaxel-resistant genes¹². Previous studies showed that PTOV1 cooperates with Zyxin to negatively regulate RA signaling. PTOV1 significantly inhibits RA-induced cancer cell cytotoxicity¹³. Shen H et al. reported that ovarian cancer was resistant to chemotherapy due to NF- κ B activation by

PTOV1¹⁴. Wu Z et al. reported that cancer stem cell characteristics are attenuated when PTOV1 levels are reduced in non-small cell lung cancer cells⁶. In MDA-MB-231 cells, PTOV1 and PIN1 knockdown shows similar anti-tumor phenotypic characteristics¹⁵. PTOV1 overexpression is correlated with tumor progression and weak prognosis in breast cancer¹⁰. Overexpression of PTOV1 is associated with esophageal squamous cell carcinoma tumorigenesis and progression¹⁶. Paciucci R et al. indicated that PTOV1 could promote the progression of prostate cancer by down-expressing the notch targets HES1 and HEY1¹⁷. PTOV1 could promote the progression of breast cancer by Wnt/ β -catenin signaling activation¹⁸. The above investigations have demonstrated that PTOV1 plays a critical role in the incidence and growth of tumors. However, its role in the progression of CRC has not been reported. Our functional experiment results also show that PTOV1 can promote the growth of CRC tumors, and both in vitro and in vivo studies have been confirmed. The above results show again that PTOV1 can promote the progression of CRC.

In order to further elucidate the mechanism of PTOV1 biological function, we used Co-IP and MS to screen the protein molecules interacting with it. After analyzing the experimental data and reviewing the literature, we finally selected the candidate protein ZNF449. Of course, we finally repeatedly used Co-IP and GST pull-down to confirm that PTOV1 and ZNF449 can be directly combined. Also, we investigated whether PTOV1 and ZNF449 co-localized with CRC cells. IF staining revealed colocalization of PTOV1 and ZNF449 in CRC cells. Additionally, immunohistochemistry revealed that PTOV1 was widely co-expressed with ZNF449 in CRC tissues. The above results all indicate that PTOV1 can directly bind ZNF449.

ZNF449 (Zinc Finger Protein 449) is a Protein Coding gene. A nuclear protein that likely serves as a transcription factor is encoded by this gene^{19,20}. Diseases associated with ZNF449 include Blue Cone Monochromacy²¹ and Fundus Dystrophy²². Gene Ontology (GO) annotations associated with this gene include the activity of DNA-binding transcription factor²³. The previous results revealed that ZNF449 has a critical role in biological processes. In order to further clarify that ZNF449 is indispensable for PTOV1 to promote CRC progression, we knocked down ZNF449 while over-expressing PTOV1 and verified it with previous functional assays. The findings revealed that overexpression of PTOV1 could promote tumor cell growth, migration, and invasion; however, knockdown of ZNF449 could reduce the enhancement of tumor cell aggressiveness caused by the up-regulation of PTOV1. These data suggest that PTOV1 promotes tumor growth through ZNF449. In addition, in order to further confirm the binding site of PTOV1 and ZNF449, we truncated and segmented PTOV1 according to the secondary results of PTOV1 and combined it with the online database prediction results. Finally, the Co-IP and GST pull-down experiment was used to verify repeatedly, and according to the experimental results, the region where ZNF449 binds to PTOV1 was finally determined. Of course, we also mutated the site where PTOV1 binds to ZNF449, and then it was confirmed by functional experiments that the disruption of PTOV1/ZNF449 interaction could slow the CRC progression.

As a common transcription factor, ZNF449 exerts its biology via regulating transcriptional activity. Using the JASPAR database⁸, we revealed that ZNF449 could possibly bind to the MYC promoter region. As the most common oncogene, MYC has been extensively declared to promote the incidence and progression of CRC^{24–27}. So as to further confirm the above findings, we used the luciferase assay, the results showed that overexpression of ZNF449 stimulated the activity of WT MYC promoter, as suggested by an increase in the activity of luciferase, but overexpression had no impact on the activity of mut-type MYC promoter. Moreover, PTOV1 enhanced the development of activity of luciferase stimulated by ZNF449. Of course, we also conducted the ChIP assay, and the outcomes showed that ZNF449 was connected to the MYC promoter and that this interaction was enhanced by PTOV1. Furthermore, the enhanced expression of ZNF449 significantly overexpressed the level of MYC protein and mRNA, both of which were further promoted by PTOV1. Interestingly, when we mutated the binding site of PTOV1 on ZNF449, we found that Δ PTOV1 failed to enhance the

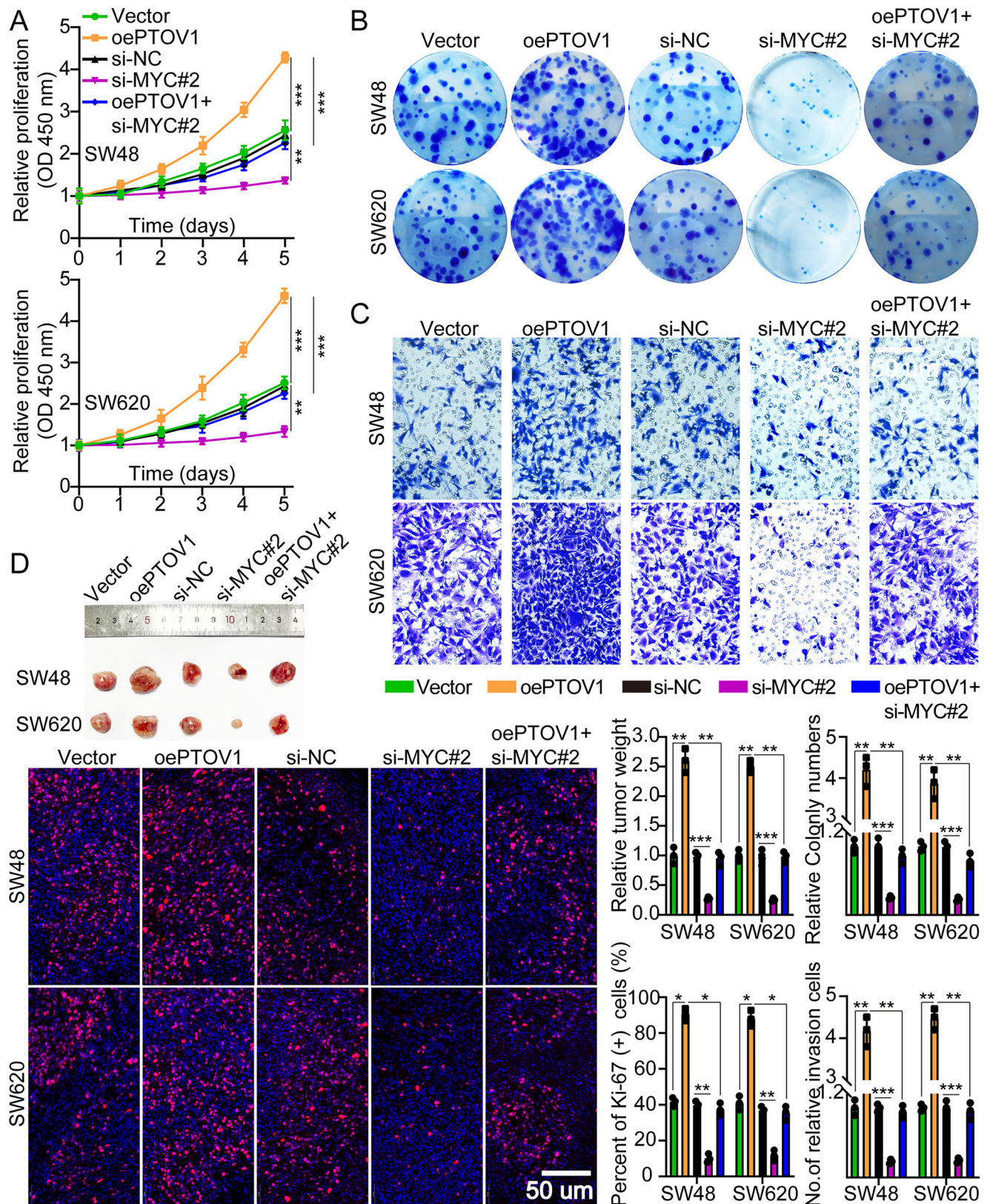


Fig. 7 | PTOV1 promotes tumor growth through MYC. A Cell growth curves measured by CCK-8 assay between Vector, oePTOV1, si-NC, si-MYC#2 and oePTOV1+si-MYC#2. **B** PTOV1 overexpression promoted colony formation and the effect could be attenuated by knock down MYC. **C** Transwell assays showing that PTOV1 overexpression promoted tumor cell invasion and the effect could be attenuated by knock down MYC. The numbers of invading cells are shown. Bars:

50 μ m. **D** Typical pictures of subcutaneous tumor between Vector, oePTOV1, si-NC, si-MYC#2, and oePTOV1+si-MYC#2. Bars: 50 μ m. The means \pm SDs are provided ($n = 3$). * $P < 0.05$, ** $P < 0.01$, and *** $P < 0.001$ according to two-tailed Student t-tests or one-way ANOVA followed by Dunnett tests for multiple comparisons.

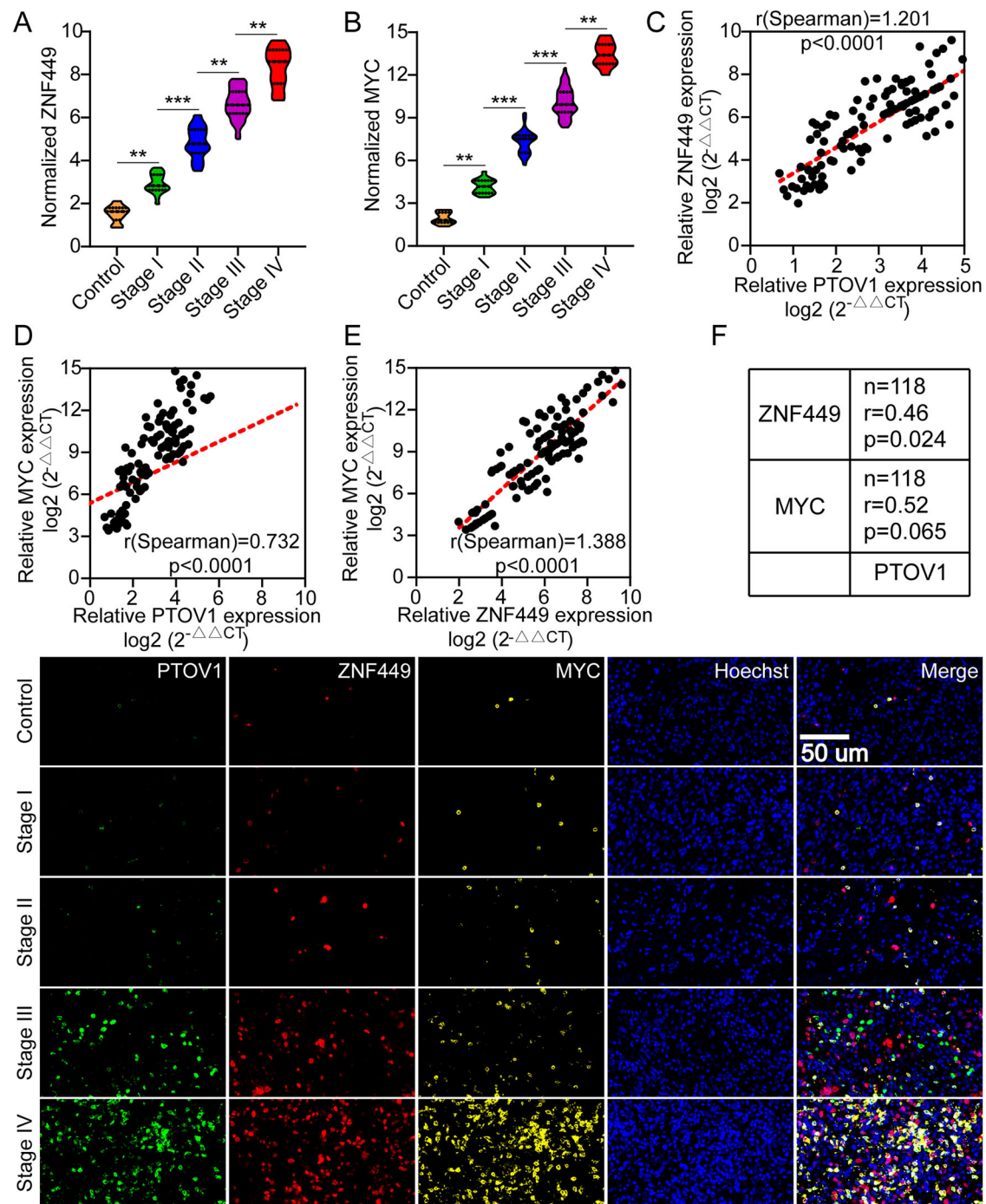


Fig. 8 | Correlation of the PTOV1/ZNF449/MYC axis with clinical progression. **A, B** Expression levels of ZNF449/MYC in normal intestinal tissue and CRC tissues by qRT-PCR. **C** Spearman correlation analysis between PTOV1 levels and ZNF449 levels in tumor tissues from CRC patients. Pearson's correlation coefficient (r) and P -value as the picture showed, $n = 118$. P -value was from Spearman's test. **D** Spearman correlation analysis between PTOV1 levels and MYC levels in tumor tissues from CRC patients. Pearson's correlation coefficient (r) and P -value as the picture showed, $n = 118$. P -value was from Spearman's test. **E** Spearman correlation

analysis between ZNF449 levels and MYC levels in tumor tissues from CRC patients. Pearson's correlation coefficient (r) and P -value as the picture showed, $n = 118$. P -value was from Spearman's test. **F** Spearman correlation analysis between PTOV1 expression levels and ZNF449 and MYC expression levels in CRC tissues. Pearson's correlation coefficient (r) and P -value as the picture showed; P -value was from Spearman's test. Scale bar represents 50 μm . The means \pm SDs are provided ($n = 3$). ** $P < 0.01$ and *** $P < 0.001$ according to two-tailed Student t -tests or one-way ANOVA followed by Dunnett tests for multiple comparisons.

elevation in the activity of luciferase stimulated by ZNF449 and enhance the binding of ZNF449 to the promoter region of MYC. These outcomes showed that ZNF449 is directly connected to the promoter region of MYC to activate its transcription, and PTOV1 promotes this process. In order to further clarify that MYC is indispensable for PTOV1 to promote CRC progression, we knocked down MYC while overexpressing PTOV1 and

verified it with previous functional assays. The outcomes revealed that overexpression of PTOV1 could promote tumor cell growth, migration, and invasion; however, knockdown of MYC could reduce the enhancement of tumor cell development, migration, and invasion caused by overexpression of PTOV1. These outcomes indicate that PTOV1 enhances tumor progression through MYC.

Finally, we identified the PTOV1/ZNF449/MYC by qRT-PCR expression level and IF among normal colorectal tissue and tumor tissue. The findings again revealed that there was a higher expression of PTOV1/ZNF449/MYC in tumor tissues, especially in Stage IV, in comparison to the expression level in Control. Additionally, the expression levels of members of the PTOV1/ZNF449/MYC signaling axis were directly proportional to one another.

This research revealed that PTOV1 is a poor predictor factor for CRC patients; it has a critical role in CRC growth, and PTOV1/ZNF449 interaction may function as a therapeutic target for CRC.

Materials and methods

Reagents and cell lines

Normal intestinal epithelium FHC and HIEC-6 cells, multiple human CRC cell lines SW1116, SW48, HCT-15, SW620, SW480, and SW1463 were cultivated according to Supplementary Materials and our prior study^{28–31}. PTOV1 was purchased from Thermo Fisher Scientific (PA5-67569). Primary antibodies were utilized to measure ZNF449 (ab236427; Abcam), MYC (ab32072; Abcam), GST (ab111947; Abcam), Flag (ab205606; Abcam), and HA (ab9110; Abcam).

CRC samples

A total of 118 samples of CRC and 10 healthy human colorectal tissues (Control) were retrieved from the Union Hospital (Wuhan, Hubei, China) from September 2018 to June 2022. All participants provided their informed approval, and the relevant research ethics committee approved the study. Before surgery, none of the patients underwent adjuvant, neoadjuvant, or radiotherapy. According to guidelines and regulations, all clinical samples and data were collected and processed. All ethical regulations relevant to human research participants were followed.

Plasmid construction and lentivirus

First, pLVX-Puro-PTOV1 overexpression plasmid was constructed. Second, expression plasmids were transfected into SW48 and SW620 cells. Our previous study describes the detailed procedure^{28,30}. Conforming to the manufacturer guidelines, SW48 and SW620 cells were regularly cultivated to 90% confluence and transfected in six-well cell culture plates. After infection, puromycin (2 µg/mL, Sigma-Aldrich, #P8833) was used to remove uninfected cells within 48 h. In order to achieve a knockout effect, we chose the two siRNAs with the highest knockout outcome according to the PTOV1, ZNF449, and MYC sequence (Table S3).

CCK-8 assay

According to the manufacturer guidelines, CCK-8 (Cell Counting Kit-8, Dojindo, Tokyo, Japan) was utilized to measure cell proliferation. A fresh medium was supplemented with a 96-well plate with 5×10^3 cells per well. The absorption rate was determined with the aid of a microplate reader (Bio-Rad Laboratories, Hercules, California, USA) following CCK-8 solution treatment. The previous publication contains more details^{28,32,33}.

Western blotting

A lysis buffer was used to lyse tissues and cells, then BCA was used to quantify them (Beyotime, Shanghai, China). The lysates were transferred to PVDF membranes after SDS-PAGE. Afterward, PVDF membranes were incubated under the appropriate conditions with antibodies and then dyed. Please refer to “Cell lines and reagents” and Table S4 for information on the primary antibody. Please refer to Supplementary Materials and our prior publication for more details^{28,30}.

Coimmunoprecipitation (Co-IP)

An immunoprecipitation procedure was performed as described in the Supplementary Materials and the published report^{29,34,35}. Cell lysates were incubated at 4 °C overnight with both IP-antibodies and Protein G-agarose beads. The precipitations and supernatants were boiled in 1% loading buffer after washing three times to prepare for western blotting.

GST pull-down assay

Similarly to our previous report²⁸, a pull-down was performed. Sepharose 4B beads (Amersham Biosciences) were used to express and purify GST-fused proteins. The purification of TAT-fused proteins was performed using Ni-Sepharose beads (Qiagen, Chatsworth, CA). At 4 °C, GST proteins were incubated with cell lysates and purified HA-ZNF449 proteins. We used GST proteins as controls. Next, immunoblotting analyses were conducted on both precipitated beads and supernatants. For more detailed information, see the supplementary material.

Real-time quantitative RT-PCR (qRT-PCR)

The assay was conducted in accordance with the manufacturer guidelines. The $2^{-\Delta\Delta Ct}$ technique normalized the GAPDH expression data, which functioned as a control. GeneCreate (Wuhan, China) synthesized the primers utilized in this research. Table S5 illustrates primer sequences.

Bioinformatic analysis

We downloaded all datasets from The Cancer Genome Atlas (TCGA) (<https://cancergenome.nih.gov/>) and Genotype-Tissue Expression (GTEx)³⁶. Independent sample t-tests comparing the two groups are represented as t-tests.

Immunohistochemistry (IHC) and Immunofluorescence (IF)

We previously reported IHC and IF details^{28,29}. As a result, the tissue was dried, embedded in paraffin, and sectioned. After that, using appropriate primary and secondary antibodies, sections were incubated. We conducted immunohistochemistry scores based on our previous study. For more detailed information, see the supplementary material.

Luciferase reporter assays

Co-transfection of various plasmids was performed on 10^5 cells/well, including an MYC-driven luciferase reporter or control plasmid encoding luciferase (Promega) on the next day. The activity of luciferase was evaluated by a luciferase reporter 36 h later (Promega, USA).

Chromatin immunoprecipitation (ChIP)

ChIP assay kits (QIAGEN) were used. Following formaldehyde crosslinking, the cells were sonicated. Incubation with anti-ZNF449 antibodies was performed after pretreatment with protein A/G beads. As a negative control, IgG was used. In this study, DNA was extracted from complexes using DNA extraction kits (QIAGEN), and quantitative real-time PCR was performed. A list of the primers used in ChIP-qPCR can be found in Table S6.

CRC growth in vivo assays

CRC growth assay in vivo was conducted as in previous reports^{28–30}. In the subcutaneous CRC mouse model, 5×10^5 CRC cells suspended in DMEM were subcutaneously injected into the nude mice at 5–6 weeks of age.

Statistics and reproducibility

Statistical analysis was performed using R 4.0.2 software (<http://www.r-project.org/>) and GraphPad Prism version 8.0 (GraphPad Inc., La Jolla, CA, USA), and statistical descriptions were presented as mean \pm SD or median (interquartile range). According to whether the data obey the normal distribution and the homogeneity of variance, the comparison between the two groups is accomplished utilizing the t-test, t' test, or rank sum test. One-way ANOVA analysis of variance, Brown-Forsythe ANOVA test, or rank sum test was utilized to compare overall means among various groups. Pairwise comparisons were performed using Dunnett, Dunnett T3, or Dunn's method for *P* value correction to control for the overall probability of type I error; two-sided *P* < 0.05 was recognized as a statistically significant difference.

Reporting summary

Further information on research design is available in the Nature Portfolio Reporting Summary linked to this article.

Data availability

The datasets generated during and/or analyzed during the current study are available from the corresponding author on reasonable request. The uncropped blot images for figures in the text are available in Figure S10. Source Data can be found in Supplementary Data 1.

Received: 14 April 2024; Accepted: 12 March 2025;

Published online: 25 March 2025

References

1. Biller, L. H. & Schrag, D. Diagnosis and treatment of metastatic colorectal cancer: a review. *JAMA* **325**, 669–685 (2021).
2. Dekker, E., Tanis, P. J., Vleugels, J. L. A., Kasi, P. M. & Wallace, M. B. Colorectal cancer. *Lancet* **394**, 1467–1480 (2019).
3. Benedit, P. et al. PTOV1, a novel protein overexpressed in prostate cancer containing a new class of protein homology blocks. *Oncogene* **20**, 1455–1464 (2001).
4. Santamaria, A. et al. PTOV-1, a novel protein overexpressed in prostate cancer, shuttles between the cytoplasm and the nucleus and promotes entry into the S phase of the cell division cycle. *Am. J. Pathol.* **162**, 897–905 (2003).
5. Santamaria, A. et al. PTOV1 enables the nuclear translocation and mitogenic activity of flotillin-1, a major protein of lipid rafts. *Mol. Cell Biol.* **25**, 1900–1911 (2005).
6. Wu, Z. et al. Depleting PTOV1 sensitizes non-small cell lung cancer cells to chemotherapy through attenuating cancer stem cell traits. *J. Exp. Clin. Cancer Res* **38**, 341 (2019).
7. Yu, Z. et al. Nitrated alpha-synuclein induces the loss of dopaminergic neurons in the substantia nigra of rats. *PLoS One* **5**, e9956 (2010).
8. Castro-Mondragon, J. A. et al. JASPAR 2022: the 9th release of the open-access database of transcription factor binding profiles. *Nucleic Acids Res.* **50**, D165–D173 (2022).
9. Morote, J. et al. PTOV1 expression predicts prostate cancer in men with isolated high-grade prostatic intraepithelial neoplasia in needle biopsy. *Clin. Cancer Res.* **14**, 2617–2622 (2008).
10. Lei, F. et al. Overexpression of prostate tumor overexpressed 1 correlates with tumor progression and predicts poor prognosis in breast cancer. *BMC Cancer* **14**, 457 (2014).
11. Rausch, S. et al. Prostate tumor overexpressed 1 expression in invasive urothelial carcinoma. *J. Cancer Res. Clin. Oncol.* **142**, 937–947 (2016).
12. Canovas, V. et al. Prostate tumor overexpressed-1 (PTOV1) promotes docetaxel-resistance and survival of castration resistant prostate cancer cells. *Oncotarget* **8**, 59165–59180 (2017).
13. Youn, H., Kim, E. J. & Um, S. J. Zyxin cooperates with PTOV1 to confer retinoic acid resistance by repressing RAR activity. *Cancer Lett.* **331**, 192–199 (2013).
14. Shen, H. et al. PTOV1 promotes cisplatin-induced chemotherapy resistance by activating the nuclear factor kappa B pathway in ovarian cancer. *Mol. Ther. Oncolytics* **20**, 499–507 (2021).
15. Karna, S. K. L., Ahmad, F., Lone, B. A. & Pokharel, Y. R. Knockdown of PTOV1 and PIN1 exhibit common phenotypic anti-cancer effects in MDA-MB-231 cells. *PLoS One* **14**, e0211658 (2019).
16. Li, R. et al. Overexpressed PTOV1 associates with tumorigenesis and progression of esophageal squamous cell carcinoma. *Tumour Biol.* **39**, 1010428317705013 (2017).
17. Alana, L. et al. Prostate tumor Overexpressed-1 (PTOV1) down-regulates HES1 and HEY1 notch targets genes and promotes prostate cancer progression. *Mol. Cancer* **13**, 74 (2014).
18. Cui, Y. et al. Prostate tumour overexpressed-1 promotes tumourigenicity in human breast cancer via activation of Wnt/beta-catenin signalling. *J. Pathol.* **239**, 297–308 (2016).
19. Ross, M. T. et al. The DNA sequence of the human X chromosome. *Nature* **434**, 325–337 (2005).
20. Huttlin, E. L. et al. Dual proteome-scale networks reveal cell-specific remodeling of the human interactome. *Cell* **184**, 3022–3040 e3028 (2021).
21. Luck, K. et al. A reference map of the human binary protein interactome. *Nature* **580**, 402–408 (2020).
22. Huttlin, E. L. et al. Architecture of the human interactome defines protein communities and disease networks. *Nature* **545**, 505–509 (2017).
23. Gaudet, P., Livstone, M. S., Lewis, S. E. & Thomas, P. D. Phylogenetic-based propagation of functional annotations within the Gene Ontology consortium. *Brief. Bioinform.* **12**, 449–462 (2011).
24. Jing, Z. et al. NCAPD3 enhances Warburg effect through c-myc and E2F1 and promotes the occurrence and progression of colorectal cancer. *J. Exp. Clin. Cancer Res.* **41**, 198 (2022).
25. Tu, R. et al. c-MYC-USP49-BAG2 axis promotes proliferation and chemoresistance of colorectal cancer cells in vitro. *Biochem. Biophys. Res Commun.* **607**, 117–123 (2022).
26. Wang, Y. N. et al. Targeting the cholesterol-RORalpha/gamma axis inhibits colorectal cancer progression through degrading c-myc. *Oncogene* **41**, 5266–5278 (2022).
27. Di, Y. et al. The c-MYC-WDR43 signalling axis promotes chemoresistance and tumour growth in colorectal cancer by inhibiting p53 activity. *Drug Resist. Update* **66**, 100909 (2023).
28. Chen, Q. et al. PIK3R3 inhibits cell senescence through p53/p21 signaling. *Cell Death Dis.* **11**, 798 (2020).
29. Chen, Q. Z., Chen, Y., Li, X., Liu, H. & Sun, X. L. TRIB3 interacts with STAT3 to promote cancer angiogenesis. *Curr. Med Sci.* **42**, 932–940 (2022).
30. Lv, Q., Xia, Q., Li, A. & Wang, Z. circRNA_101277 influences cisplatin resistance of colorectal cancer cells by modulating the miR-370/IL-6 axis. *Genet. Res.* **2022**, 4237327 (2022).
31. Lv Q., Xia Q., Li A., Wang Z. The potential role of IL1RAP on tumor microenvironment-related inflammatory factors in stomach adenocarcinoma. *Technol. Cancer Res. Treat.* **20**, 1533033821995282 (2021).
32. Li, J. et al. Hypoxic glioma stem cell-derived exosomes containing Linc01060 promote progression of glioma by regulating the MZF1/c-Myc/HIF1alpha axis. *Cancer Res.* **81**, 114–128 (2021).
33. Li, J., Yuan, H., Xu, H., Zhao, H. & Xiong, N. Hypoxic cancer-secreted exosomal miR-182-5p promotes glioblastoma angiogenesis by targeting Kruppel-like factor 2 and 4. *Mol. Cancer Res.* **18**, 1218–1231 (2020).
34. Li, J. et al. ELTD1 facilitates glioma proliferation, migration and invasion by activating JAK/STAT3/HIF-1alpha signaling axis. *Sci. Rep.* **9**, 13904 (2019).
35. Wang, Z. et al. MRPS16 facilitates tumor progression via the PI3K/AKT/Snail signaling axis. *J. Cancer* **11**, 2032–2043 (2020).
36. Consortium GT. The Genotype-Tissue Expression (GTEx) project. *Nat. Genet.* **45**, 580–585 (2013).

Acknowledgements

This work was supported by the Natural Science Foundation of Hubei, China (No. 2021CFB108). The authors thank Home for Researchers editorial team (www.home-for-researchers.com) for language editing service.

Author contributions

All authors contributed to the study conception and design. Material preparation was performed by Zhi-yong Wang, Qianzhi Chen, Xinwei Qiao, and An-shu Li, data collection and analysis were performed by Ka-ming Xue and Qianzhi Chen. The first draft of the manuscript was written by Zhi-yong Wang, Xinwei Qiao, and An-shu Li. All authors participated in revising the manuscript. All authors read and approved the final manuscript.

Competing interests

The authors declare no competing interests.

Ethical approval and consent to participate

Tongji Medical College of Huazhong University of Science and Technology Ethics Committee approved all aspects of the study with informed consent from all patients. Tongji Medical College's Institutional Animal Care and Research Advisory Committee approved all animal experiments conducted in the laboratory.

Consent for publication

All authors who have contributed to the study agree to publish it.

Additional information

Supplementary information The online version contains supplementary material available at <https://doi.org/10.1038/s42003-025-07930-2>.

Correspondence and requests for materials should be addressed to Qianzhi Chen or Anshu Li.

Peer review information *Communications Biology* thanks the anonymous reviewers for their contribution to the peer review of this work. Primary Handling Editor: Christina Karlsson Rosenthal. A peer review file is available.

Reprints and permissions information is available at <http://www.nature.com/reprints>

Publisher's note Springer Nature remains neutral with regard to jurisdictional claims in published maps and institutional affiliations.

Open Access This article is licensed under a Creative Commons Attribution-NonCommercial-NoDerivatives 4.0 International License, which permits any non-commercial use, sharing, distribution and reproduction in any medium or format, as long as you give appropriate credit to the original author(s) and the source, provide a link to the Creative Commons licence, and indicate if you modified the licensed material. You do not have permission under this licence to share adapted material derived from this article or parts of it. The images or other third party material in this article are included in the article's Creative Commons licence, unless indicated otherwise in a credit line to the material. If material is not included in the article's Creative Commons licence and your intended use is not permitted by statutory regulation or exceeds the permitted use, you will need to obtain permission directly from the copyright holder. To view a copy of this licence, visit <http://creativecommons.org/licenses/by-nc-nd/4.0/>.

© The Author(s) 2025